OPERATION CHARACTERISTICS OF EXTERNAL HEAT EXCHANGERS IN THE 600MW SUPERCRITICAL CFB BOILER

Runxia Cai[1], Xin Mo[1], Junfu Lv[1], Hairui Yang[1]*, Xiujian Lei[2], Wen Ling[2], Hu Su[3], Qi Zhou[3]

[1] *Department of Thermal Engineering，Tsinghua University，Beijing，China*
[2] *Sichuan Baima Circulating Fluidized Bed Exampled Power Limited Liability Company，Neijiang，China*
[3] *Dongfang Boiler Group Co. Ltd，Chengdu，China*
*Email: yhr@mail.tsinghua.edu.cn

Abstract –A series of experiments were conducted to obtain the actual operation characteristics of external heat exchangers (EHEs) in the 600MW supercritical CFB boiler. The operation of EHEs on bed temperature, the bed-to-surface heat transfer coefficients and tube wall temperature distribution in EHEs were studied in this paper. The results show that by controlling the solid flow rates to the EHEs, furnace temperature can be adjusted for good performance at various boiler loads. And the tube panel wall temperatures are found to be a saddle-shaped distribution, which is high in the bed center but low near the wall. Packet renewal theory is used to explain such uneven temperature distribution.

INTRODUCTION

Circulating fluidized bed (CFB) Technology has developed rapidly in recent decades for its good fuel flexibility, effective NOx formation control and high-sulfur capture efficiency. With the CFB unit capacity increasing, the furnace volume increases faster than the enclosing heat transfer surface, so more heating surfaces are required to be added into the solid circulation loop to control the furnace temperature (Marchetti et al. 2003). The external heat exchanger is one of the most common used equipment to realize it. Previous studies (Goidich et al., 1999 and Xiong et al., 2010) have shown that EHEs provide great convenience for furnace temperature and steam parameters regulation by controlling the solid flow rate to the EHEs, which will be beneficial for CFB boilers to adapt to various fuels and boiler loads. In addition, as for the stable furnace temperature between 850 and 900 °C, the EHE is also important for SO_2 and NOx emission control (Zhang et al., 2012).

For supercritical and ultra-supercritical CFB boilers, external heating surfaces must be arranged for additional boiler heat duty. Although many experimental research were carried out on the performance of EHEs in laboratorial and small-scale CFB boilers (Wang et al., 2003), the reports about the actual operation of external heat exchangers in supercritical CFB boilers were few. Most literatures focused on the overall operating performance of EHEs, but with little consideration on the local gas-solid flow and heat transfer in EHEs (Werderman et al., 1993 and Wang et al., 2015). However, in order for a better adjustment for furnace temperature and steam parameters, the local gas-solid flow in EHEs should be studied.

The first 600MW supercritical CFB boiler was constructed and put into commercial operation in Neijing, Sichuan Province in China (Li et al., 2010 and Yue et al., 2015). The pant-legs structure is adopted in this unit, which has twin air distributors and twin furnaces with a common water wall between them. The thermal circulating loop with EHEs of 600MWe CFB boiler is shown in Fig.1. Six cyclones, six EHEs and six loopseals are arranged on two sides of the furnace, with three sets on each side. The design parameters are listed in Table 1. After a period of operation, although EHEs have shown many advantages for boiler operation, the tube wall temperatures are found to be a saddle-shaped distribution which is high in the bed center but low near the wall. So the present work attempts to measure the parameters in the 600MW CFB boiler, analyze the actual operation characteristics of EHEs and explain the uneven tube wall temperature distribution.

Table 1. The design parameters of 600MW CFB boiler

Item	Unit	Value
Boiler load	MWe	600
Steam Output	t/h	1900
Superheated Steam Temperature	°C	571
Superheated Steam Pressure	MPa	25.4
Reheat Steam Temperature	°C	569
Reheat Steam Pressure	MPa	4.149

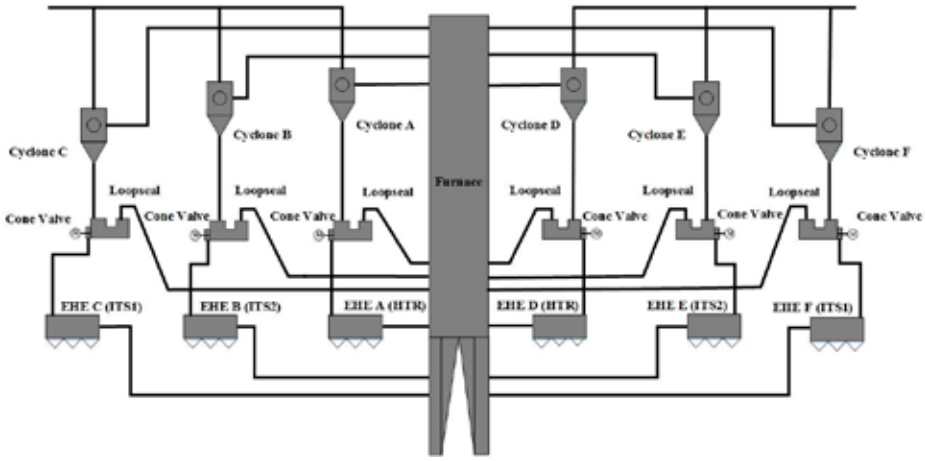

Fig.1 Thermal circulating loop with EHEs of 600 MW CFB boiler.

EXPERIMENTAL SETUP

Configuration of the EHE

As shown in Fig.1, two intermediate temperature superheaters (ITS1 and ITS2) and a high temperature reheater (HTR) are respectively immersed in the EHEs on each side. HTR is located in EHE A or D besides the front wall, ITS1 in EHE C or F besides the rear wall, and ITS2 in EHE B or E at the middle (Yue et al., 2008). Each EHE has individual solid ash inlet and outlet, which linked to the loopseal and the furnace, respectively. By means of controlling the cone valves between loopseals and EHEs, the certain rate of solids collected by the cyclones are introduced to EHEs to regulate the heat transfer between high temperature ash and immersed tubes, so as to control the steam temperature.

The EHE is actually a small bubbling bed, which is typically divided by water-cooled partitions into two chambers. The first chamber is the overflow chamber, and the second one is the heat transfer chamber. Solids enter into the first chamber through an orifice in the side wall, then overflow the partition to the heat transfer chamber, and outflow after transferring heat to tubes. The solid flow direction is parallel to the heating surface in the 600MW CFB boiler, which is different from that in 300MW CFB boiler in Baima. Fluidizing air is introduced to chambers through independent wind box and air distributor. Both the solid flow rate and the fluidizing air can control the ash temperature in EHEs. The average particle diameter of the circulating ash is ranging from 0.2 to 0.5mm, and the air velocity is between 0.3-0.5 m/s. Due to the low air velocity and small particle size, the severe abrasion of heating surface can be avoided in EHE (Zhang et al, 2012).

Methodology and Experiments

In order to investigate the effects of EHE on bed temperature, 40 thermocouples were installed at 5 different furnace heights to obtain the furnace temperature distribution, which are 0.3m, 0.7m, 1.2m, 9m and 46m above air distributor, respectively. Additionally, to obtain the operation characteristics of EHEs, solids temperature, fluidizing air rate, and steam parameters in EHEs are measured. The net dimension of EHE is 5.0m in width, and 5.7m in length, and the water-cooled partition between the first and second chamber is 3.3m in height. Wear-resisting thermocouples are used to measure the solid temperatures at the inlet and outlet of heat transfer chamber in each EHE. The flow meters and thermocouples are installed at the air entrance of each chamber to measure the air flow rate. And according to the pressure and temperature measurement of steam at inlet and outlet of each heating surface in EHE, steam enthalpy can be obtained. Besides, shielded thermocouples were installed at the outlet wall of tube panels in EHE, covered by high heat-insulating materials. Since the thermal conductivity of tube wall material is much higher than that of the heat insulating material, the measured wall temperature can represent the outlet steam temperature of corresponding tube panel.

Three experimental conditions, stable loads at 600MWe , 365MWe and variable load from 380MW to 600MW, were studied during the test. To avoid the fluctuation of measured data, all the measurement results are averaged for the following calculation and analysis.

Therefore, through the heat balance equation, the solid mass flow rate in EHE can be calculated by the following Eq. (1)

$$m_{ash} = \frac{Q_{ash}}{\Delta h_{ash}} \tag{1}$$

where m_{ash} is the ash mass flow rate to EHE, Q_{ash} is the heat release of ash, and Δh_{ash} is the enthalpy difference of ash between the inlet and outlet of EHE. Q_{ash} can be calculated from Eq. (2)

$$Q_{ash} = Q_{steam} + Q_{air} \tag{2}$$

where Q_{steam} is the heat absorption of steam, and Q_{air} is the heat absorption of air. These two terms can be obtained by Eqs. (3) and (4),

$$Q_{steam} = m_{steam}(h_{steam,out} - h_{steam,in}) \tag{3}$$

$$Q_{air} = m_{air}(h_{air,out} - h_{air,in}) \tag{4}$$

where m_{steam} and m_{air} are the mass flow rate of steam and air, $h_{steam,out}$ and $h_{steam,in}$ are the steam enthalpy at the inlet and outlet of heating surface; $h_{air,out}$ and $h_{air,in}$ are the air enthalpy at the inlet and outlet of EHE respectively.

Also the bed-to-wall heat transfer coefficient h_t can be calculated in the similar way by the following Eq. (5),

$$h_t = \frac{Q_{steam}}{A\Delta t} \tag{5}$$

where A is the total heating surface area in EHE; Δt is the log-mean-temperature difference, which is defined by Eq. (6):

$$\Delta t = [(T_{ash,in} - T_{steam,out}) - (T_{ash,out} - T_{steam,in})] / \ln \frac{T_{ash,in} - T_{steam,out}}{T_{ash,out} - T_{steam,in}} \tag{6}$$

RESULETS AND DISCUSSION

The effects of EHE on furnace temperature at variable load conditions

In order to evaluate the regulation of EHE on furnace temperature at variable load conditions, bed temperature distribution was measured at different boiler loads. Some data points near the secondary air inlet, which were obviously lower than the others, were not used in data processing. The bed temperature distribution of the left and right sides of the pant-legs furnace at different loads are shown in Fig. 2. The furnace temperature decreased with height because of the decaying solid suspension density along the furnace height. The heating surface area increased with height, while the combustible matters and the heat release both decreased with the solid concentration. Therefore, the furnace temperature was higher in the dense zone, but lower in the dilute zone. The relatively higher temperature in the upper part of dilute zone might be due to the solid rebound from the furnace roof and thicker insulation layer at the entrance of cyclone. There were only small temperature differences between two sides of furnace at different boiler loads. And the temperature in the dilute zone was well distributed in two sides, especially in the upper part. And the bed temperatures had no significant change with the load changing from 380MWe to 600MWe.

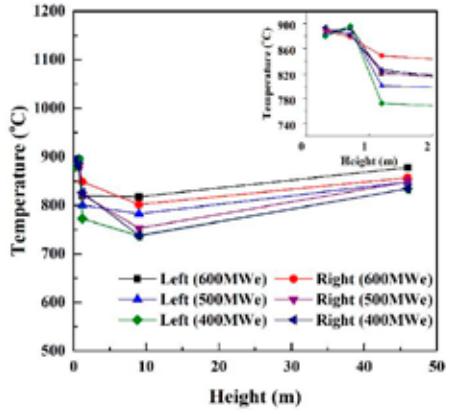

Fig.2 Furnace temperature distribution at different boiler loads

For the cooling effect of primary and secondary air, the middle part of the dense bed with the relatively stable temperature is used to represent the bed temperature. At variable load conditions, the period of boiler load increasing from 380 MWe to 600 MWe was 20 hours. Time variations of the load and the bed temperatures in twin furnace are shown in Fig. 3, and time variations of valve opening are shown in Fig. 4. With load increasing, bed temperature was controlled in a range between 850 °C and 900 °C. The bed temperature of left side is about 890 °C, and that of the right side is about 875 °C. Such temperature difference might be due to the non-uniformed combustion in furnace caused by the secondary air and the feeding coal. Although there was some fluctuation in the variable load process, bed temperatures of both sides were relatively stable. The valve opening and the bed temperature varied in a similar trend in these two figures. For instance, during the period from 5 to 7 hours, there was a steep drop of bed temperature of right side. The valve opening of E and F was rapidly decreased to reduce the proportion of ash to EHEs, so that the bed temperature could be back to normal value. However, from 7 to 10 hours, the bed temperature increased rapidly followed by a considerably increase of valve opening. So the stable bed temperature was attributed to the regulation of EHEs. The valve opening simultaneously varied with bed temperature in order to maintain the stable bed temperature.

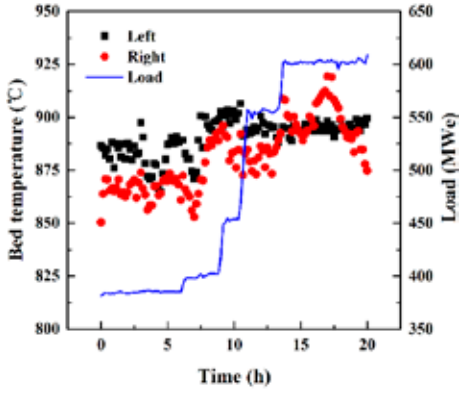

Fig.3 The variation of bed temperature with load

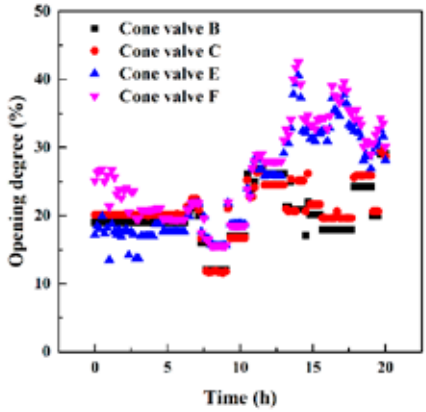

Fig.4 The time variation of valve opening

The heat transfer coefficient of different heating surface in EHEs

Steam, air and ash parameters at 365 MWe and 600 MWe are listed in Tables. 2 and 3. And the heating absorption and heat transfer of different heating surfaces in EHEs, solid flow rates to EHEs are calculated by the method mentioned above. The calculation results are listed in Tables. 4 and 5. Compared with EHE B, C, E and F, the ash flow rates to EHE A and D were much higher at partial load condition. As HTR is installed in EHE A and D, the relatively high ash flow rate ensures the outlet reheat steam temperature stable.

At 365 MWe, the heat transfer coefficients in EHE A, B, C, D, E and F were 208, 145, 271, 220, 145, 160 W/(m^2·°C), respectively. And at 600MWe load, the heat transfer coefficients increased to 232, 173, 224, 227, 198, 197 W/(m^2·°C). As average heat transfer coefficients in furnace is usually much lower than 200 W/(m^2·°C), the high average heat transfer coefficient in the EHEs enhances the utilization rate of heating surface (Basu et al., 1996). And such a big range of heat transfer coefficients also provides great convenience for adjusting steam and ash temperatures.

Table.2 Steam, air and ash parameters at 365 MWe

Parameters	Units	EHE A (HTR)	EHE B (ITS Ⅱ)	EHE C (ITSI)	EHE D (HTR)	EHE E (ITS Ⅱ)	EHE F (ITSI)
Steam flow	kg/s	124.18	144.25	143.84	124.19	144.94	144.94
Inlet steam temperature	°C	456.51	465.08	436.18	455.11	461.49	439.60
Outlet steam temperature	°C	552.58	488.57	468.61	550.94	483.64	464.16
Inlet steam pressure	Mpa	2.42	25.17	25.30	2.42	25.21	25.33
Air flow	kg/s	5.51	3.00	3.00	4.31	4.13	3.17

Inlet ash temperature	℃	830.30	799.27	798.30	819.08	805.15	808.31
Outlet ash temperature	℃	650.42	558.69	498.49	631.64	543.84	553.85

Table.3 Steam, air and ash parameters at 600 MWe

Parameters	Units	EHE A (HTR)	EHE B (ITS Ⅱ)	EHE C (ITSI)	EHE D (HTR)	EHE E (ITS Ⅱ)	EHE F (ITSI)
Steam flow	kg/s	193.68	231.18	224.35	193.37	233.23	225.55
Inlet steam temperature	℃	464.75	478.71	454.08	464.86	475.75	453.42
Outlet steam temperature	℃	547.12	510.25	483.26	546.43	510.09	485.41
Inlet steam pressure	Mpa	4.08	25.16	25.29	4.08	25.17	25.29
Air flow	kg/s	4.64	2.96	3.00	5.59	2.97	3.03
Inlet ash temperature	℃	882.35	889.73	852.21	890.11	866.16	875.83
Outlet ash temperature	℃	712.31	708.98	598.66	712.00	705.49	676.42

Table.4 Heat balance at 365 MWe

Items	Units	EHE A (HTR)	EHE B (ITS Ⅱ)	EHE C (ITSI)	EHE D (HTR)	EHE E (ITS Ⅱ)	EHE F (ITSI)
Absorbed heat by steam	kW	31336.92	14438.96	23921.29	31252.24	14045.03	18306.37
Absorbed heat by air	kW	3991.08	1915.37	1814.65	2977.06	2614.69	2033.40
Heat released by ash	kW	35328.00	16354.33	25735.93	34229.30	16659.72	20339.77
Ash flow rate	kg/s	216.62	75.26	95.26	201.58	70.61	88.49
Heat coefficient	$W/(m^2 \cdot ℃)$	207.57	145.08	271.00	220.39	145.43	159.65

Table.5 Heat balance at 600 MWe

Items	Units	EHE A (HTR)	EHE B (ITS Ⅱ)	EHE C (ITSI)	EHE D (HTR)	EHE E (ITS Ⅱ)	EHE F (ITSI)
Absorbed heat by steam	kW	36973.76	28388.56	29524.07	36565.58	31438.94	32410.87
Absorbed heat by air	kW	3643.03	2300.61	2073.58	4352.22	2258.36	2273.37
Heat released by ash	kW	40616.79	30689.16	31597.65	40917.80	33697.30	34684.24
Ash flow rate	kg/s	262.82	186.81	137.60	252.73	230.86	191.54
Heat coefficient	$W/(m^2 \cdot ℃)$	232.47	172.81	224.13	227.09	198.27	197.13

Tube Wall Temperature Characteristic of EHE

Tube wall temperature distributions of heating surfaces in EHEs at 600MWe are shown in Figs. 4(a) and 4(b). The x coordinate represents the dimensionless position in width, which is perpendicular to the ash flow direction, and value x= 0 and 1 are the internal boundaries of EHEs. Each data point in figures represents a tube panel. Since there are nearly 40 tube panels in width, only 11 representative panels are shown in Fig. 4. The wall temperatures of tube panels are found to be a saddle-shaped distribution which is high in the bed center but low near the wall. The temperature differences of HTR, ITSI, and ITS Ⅱ are 80 °C, 40 °C, and 40 °C, respectively.

The temperature deviation of HTR is more serious than that of ITSI and ITS Ⅱ. Although highest wall temperature of tube panel is still within the allowable temperature range of tube material now, it will be much worse in some cases, such as ultra-supercritical CFB boiler. As the reheat steam temperature is set to be 620 °C or even higher, the temperature deviation will result in tube burst and even forced outage. So such uneven temperature distribution should be well studied for the development of ultra-supercritical CFB boiler in the future.

The tube panel in EHEs has the serpentine structure, which can be regarded as a combination of several vertical pipes and horizontal pipes. So previous studies on heat transfer and surface hydrodynamics of a vertical pipe and horizontal pipe in the fluidized bed can be used for reference. In bubbling fluidized beds, it is commonly recognized that there are three types of mechanisms contributing to the bed to surface heat transfer, including radiation, gas convection and particle convection. As particle density is so high in bubbling beds, the particle convection is regarded as dominated. Particle convection is caused by the bubble-wake induced

movement (Melerus et al, 1992), which is the predominant mechanism in bubbling bed. Pister et al (2011), Stefanova et al. (2011) and Vreedenberg et al. (1958) investigated the radial variations of heat transfer coefficients in cylinder bubbling fluidized bed. And all of them have found that the heat transfer coefficients are higher in the central region than near the wall region, which is attributing to the additional turbulence caused by large bubbles moving in the central region. And Pister et al. (2011) and Yao et al (2015) used the packet renewal theory (Mickley and Fairbanks, 1955) to coordinate the heat transfer coefficients. Root-square-average residence time and packet fraction are the two surface hydrodynamics parameters in the packet renewal theory. The longer the residence time indicates the lower renewal frequency of packet, resulting in lower heat transfer coefficients. And the higher packet fraction leads to the higher heat transfer coefficient. Yao et al (2015) found that the packet residence time increased from bed central region to wall region and the packet residence time played a more dominant role than packet fraction on heat transfer.

With respect to the tube wall temperature deviation in EHEs, the bubble possibility or the packet renewal frequency can be used to explain the heat transfer deviation. Due to the effect of wall friction and bubble coalescence, although the bubbling possibility is relatively uniform near air distributor, it will show a clearer distribution in a higher height. The bubble possibility is much higher in the central region than in the wall region (Hernández-Jiménez et al, 2011). So higher turbulence in the center caused by the fast bubbles leads to a higher heat transfer coefficient, resulting in higher heat absorption by steam. And the tube panel wall temperature is higher in the center but lower near the wall.

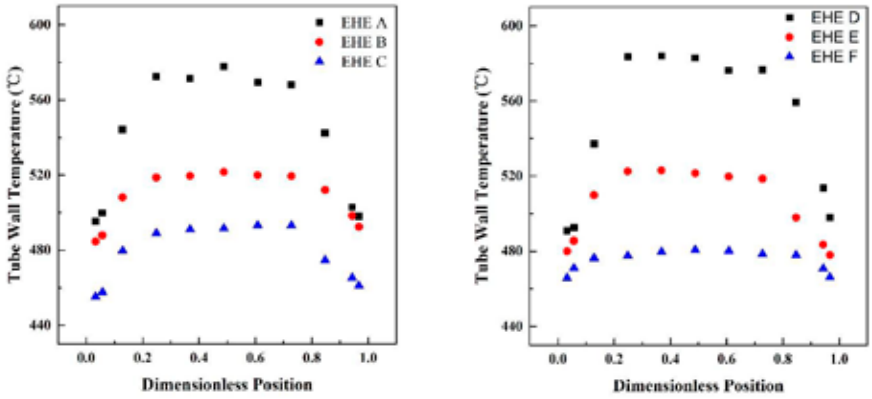

(a) EHE A, B, C (a) EHE D, E, F

Fig. 5 Tube wall temperature distribution versus dimensionless position

CONCLUSIONS

EHE provides great convenience for the controlling on bed temperature and steam parameters. Three groups of experiments were conducted to obtain the actual operation characteristics of external heat exchangers (EHEs) in the 600MW supercritical CFB boiler. By controlling the solid flow rates to the EHEs, bed temperature can be adjusted for good performance under various boiler loads. And such effective control can be attributed to the high heat transfer coefficients of heating surfaces in EHEs. The tube panel wall temperatures are found to be a saddle-shaped distribution, which is high in the bed center but low near the wall. Packet renewal theory is used to explain such uneven temperature distribution. This non-uniformed heat transfer phenomenon needs intensive study in the future.

ACKNOWLEDGEMENT

Financial support of this work by Key Project of the National Thirteen-Five Year Research Program of China (2016YFB0600203).

NOTATION

A	heat absorption surface area, m^2
m_{ash}	ash mass flow rate to EHE, kg/s
m_{steam}	steam mass flow rate, kg/s
m_{air}	air mass flow rate, kg/s
$h_{air,in}$	air enthalpy at the outlet, kJ/kg
$h_{air,out}$	air enthalpy at the outlet, kJ/kg
Δh_{ash}	enthalpy difference of ash, kJ/kg
$h_{steam,out}$	steam enthalpy at the outlet, kJ/kg
$h_{steam,in}$	steam enthalpy at the inlet, kJ/kg
h_t	heat transfer coefficient, W/(m^2·°C)
Q_{ash}	heat release of ash, kJ
Q_{steam}	heat absorption of steam, kJ
Q_{air}	heat absorption of air, kJ
$T_{ash,in}$	ash temperature at the inlet, °C
$T_{ash,out}$	ash temperature at the inlet, °C
$T_{steam,in}$	steam temperature at the inlet, °C
$T_{steam,out}$	steam temperature at the outlet, °C
EHE	external heat exchanger
HTR	high temperature reheater
ITS	intermediate temperature superheater

REFERENCES

Basu, P., & Nag, P. K. 1996. Heat transfer to walls of a circulating fluidized-bed furnace. Chemical Engineering Science, 51(1), 1-26.

Goidich, Stephen J., Timo Hyppanen, and Kari Kauppinen. 1999. CFB boiler design and operation using the INTREXTM heat exchanger. 6th International Conference on Circulating Fluidized Beds, Würzburg, Germany. 1999.

Hernández-Jiménez, Fernando, et al. "Comparison between two-fluid model simulations and particle image analysis & velocimetry (PIV) results for a two-dimensional gas–solid fluidized bed." Chemical engineering science 66.17 (2011): 3753-3772.

Li, Y., Nie, L., Hu, X., Yue, G., Li, W., We, Y., ... & Che, D. 2009. Structure and performance of a 600MWe supercritical CFB boiler with water cooled panels. In Proceedings of the 20th International Conference on Fluidized Bed Combustion (pp. 132-136). Springer Berlin Heidelberg.

Marchetti, M. M., Czarnecki, T. S., Semedard, J. C., Devroe, S., & Lemasle, J. M. 2003. Alstom's large CFBs and results. In 17th International Conference on Fluidized Bed Combustion (pp. 673-683). American Society of Mechanical Engineers.

Melerus O, Mattmann W. 1992. Heat transfer mechanisms in gas fluidized beds. Part 1: Maximum heat transfer coefficients, Chemical Engineering and Technology, 15(3): 139-150.

Mickley, H., Fairbanks, D. 1955. Mechanism of heat transfer to fluidized beds. AIChE Journal, 1(3), 374-384.

Pisters, K., Prakash, A. 2011. Investigations of axial and radial variations of heat transfer coefficient in bubbling fluidized bed with fast response probe. Powder Technology, 207(1), 224-231.

Stefanova, A., Bi, H., Lim, J., Grace, J. 2011. Local hydrodynamics and heat transfer in fluidized beds of different diameter. Powder technology, 212(1), 57-63.

Vreedenberg, H. 1958. Heat transfer between a fluidized bed and a horizontal tube. Chemical Engineering Science, 9(1): 52-60.

Wang, H., Lu, X., Zhang, W., Wang, Q., Chen, J., Kang, Y., ... and Xie, X. 2015. Study on heat transfer characteristics of the high temperature reheater tube panel in a 300 MW CFB boiler with fluidized bed heat exchanger. Applied Thermal Engineering, 81, 262-270.

Wang Q., Luo Z., Fang M., Ni M., Cen K. 2003. Development of a new external heat exchanger for a circulating fluidized bed boiler. Chemical Engineering and Processing: Process Intensification, 42(4), 327-335.

Werderman, C., Werther, J. 1993. Solids flow pattern and heat transfer in an industrial-scale fluidized bed heat exchanger. Proceeding of 12th Int. Conf. Fluidized Bed Combustion. 985-990.

Xiong B, Lu X, Amano R, Liu H et al. 2012. Gas–solid flow in an integrated external heat exchanger for CFB boiler. Powder Technology, 202(1). 55-61.

Yao, X., Zhang, Y., Lu, C., Han, X. 2015. Systematic study on heat transfer and surface hydrodynamics of a vertical heat tube in a fluidized bed of FCC particles. AIChE Journal, 61(1), 68-83.

Yue, G., Yang, H., Nie, L., Wang, Y., and Zhang, H. 2008. Hydrodynamics of 300 MWe and 600 MWe CFB boilers with asymmetric cyclone layout. Circulating Fluidised Bed Technology IX, 13-16.

Yue, G., Ling, W., Lu, J., Yang, H., Xiao, C., Nie, L., Su, H. 2015. Development and Demonstration of the 600 MW Supercritical CFB Boiler in Baima Power Plant, 22nd International Conference on Fluidized Bed Combustion, Turku, Finland, 126-134

Zhang M, Wu H, Lu Q, Sun Y, Song G. 2012. Heat transfer characteristics of fluidized bed heat exchanger in a 300MW CFB boiler. Powder technology, 222. 1-7.